Hindawi
International Journal of Aerospace Engineering
Volume 2017, Article ID 4164260, 10 pages
https://doi.org/10.1155/2017/4164260

Research Article

Analytical Approach for Orbital Evasion with Space Geometry Considered

Dateng Yu,[1] Hua Wang,[1] Shuai Guo,[1] and Hongyu Wang[2]

[1] *College of Aerospace Science and Engineering, National University of Defense Technology, Changsha, China*
[2] *Aerospace System Engineering Shanghai, Shanghai 200000, China*

Correspondence should be addressed to Hua Wang; wanghua@nudt.edu.cn

Received 6 December 2016; Revised 23 January 2017; Accepted 15 February 2017; Published 8 March 2017

Academic Editor: Heidi Kuusniemi

This paper researches an optimal problem of orbital evasion with considering space geometry by using an analytical approach. Firstly, an angles-only relative navigation model is built and the definition of completely nonobservable maneuver is proposed. After algebraic analysis of relative space geometry, it is proved that the completely nonobservable maneuver is nonexistent. Based on this, the angle measurements of orbit without evasion are set as reference measurements and an analytical solution is derived to find the minimum difference between measurements and the reference measurements in a constant measuring time. Then, an object function using vector multiplication is designed and an optimization model is established so as to prove the optimality of analytical solution. At last, several numerical simulations are performed with different maneuver directions, which verify the effectiveness of the analytical method of this paper for orbital evasion problem. This method offers a new viewpoint for orbital evasion problem.

1. Introduction

Nowadays the satellites face various threats, not only orbit debris but also some noncooperative rendezvous. To increase the survivability of satellites, it is important to have some evasion strategies and perform optimally evasive maneuvers. In this paper, we focus on optimal evasion strategies for an evading satellite against a noncooperative rendezvous spacecraft. It should be mentioned that both of the relevant spacecrafts are active-spacecraft, and the debris is out of consideration in this paper.

The optimal evasion problem has been studied for many years [1–6]. In this problem, a pursuer tries to approach its target (namely, an evader) through several evasive maneuvers, at the same time the evader expects to escape from the pursuer through some optimal evasive maneuvers. Varieties of evasion strategies had been proposed. Shinar and Steinberg [7] proposed a closed form expression for a switching equation with a new navigation gain considered. Forte et al. [8] analyzed an equivalent linearization of the three-dimensional optimal avoidance problem.

The optimal evasive strategies have been applied on many aerospace problems. Kelly and Picciotto [9] proposed an optimal rendezvous evasive method by using a nonlinear optimization technology. Patera [10–12] firstly introduced an optimal evasive strategy in consideration of collision probability. Bombardelli [13] obtained an optimal maneuver method to numerically maximize the miss distance, which described the arc length separation between the maneuvering rear point and the predicted collision point. Recently, the study of evasive maneuvers has been done with different emphasis, Lee et al. [14, 15] used genetic algorithm to find a solution of minimum fuel consumption and to determine delta-V maneuvers in LEO and GEO. de Jesus and de Sousa [16] investigated the existence of symmetry in determining the initial conditions of collisions among objects. The evasion problem studies mentioned above did not consider the navigation performance influence. In addition, the approaching objects were always considered to be debris or failure vehicles in most of the orbital evasion research, which means that the evasion strategy may be useless when the object is changed to noncooperative spacecraft.

In fact, the navigation performance is actually a significant view to analyze evasion strategies. In this paper, we introduced space geometry of the two spacecraft in an orbital evasion problem to characterize the measurements as a new index. As known, the system observability can be altered by the maneuvers of evader and pursuer during angles-only navigation [17, 18]. Vallado [19] found that the diversity of relative motion had a positive nonlinear correlation with the system observability. Woffinden and Geller [20] derived an analogical correlation between system observability and maneuvers in the orbit rendezvous field. Grzymisch and Fichter [21, 22] found an optimal maneuver method for rendezvous through analyzing the observability conditions. Dateng et al. [23] used a multiobjective optimization approach to investigate orbital evasion problem with the consideration of system observability. The fundamental reason why the system observability can be altered by the maneuvers of evader and pursuer is that these maneuvers alter the relative space geometry and the measurements that the pursuer and the evader can acquire. This is the viewpoint which this paper tried to focus on.

In this work, a novel analytical evasion strategy is proposed to find optimal evasive maneuvers by considering the variation of relative space geometry and measurements. The rest of this paper is organized as follows. First, a problem overview about the orbital evasion is described. Then, an angles-only relative navigation model is established and the definition of completely nonobservable maneuver is proposed. After algebraic analysis of relative space geometry, it is proved that the completely nonobservable maneuver is nonexistent. Based on this, an analytical solution is derived to find the optimal evasive maneuver. Then, an optimization model is established and numerical solution using genetic algorithm (GA) is introduced so as to prove the optimality of analytical solution. At last, a numerical simulation is performed to verify the validity of the method. The results indicate that the analytical method proposed in this paper can reach the expected effect.

2. Problem Overview

There are usually two spacecrafts in an orbital evasion problem (a pursuer and an evader). The objective of pursuer is to capture or approach the evader, and the objective of evader is to find some evasion strategies and escape by the pursuer. This paper researches the optimal evasion strategy when the initial relative distance is about 100 km and the initial orbits are coplanar and HEO (Highly Elliptical Orbit).

At such distance, the pursuer usually only has two angle measurements, because the evader is noncooperative and the LiDAR (Light Detection and Ranging) cannot get distance measurements in such a range. Assuming that evader and pursuer both know the initial state of each other, the pursuer will acquire the future state of evader through angle measurements with the help of some filters. The angle measurements of orbit without evasion are set as reference measurements. Generally, the angle measurements will have a great change when the evader starts an evasive maneuver, meaning that pursuer can catch the maneuver through filtering immediately. When pursuer gains the evasive maneuver, it can replan its approaching to make the evasive maneuver invalid.

However, if the evasive maneuver causes minor or even no difference in angle measurements compared with the reference measurements, the accuracy of filtering will be declined or even non convergent. Thus, the accuracy of navigation has a relationship with the relative space geometry which is influenced by the evasive maneuver. In this way, the evasive maneuver can change the accuracy of navigation and the system observability.

The optimal evasive maneuver is expected to minimize the difference of angle measurements pursuer acquired between evasion and no evasion, and then the difficulty of filter tracking is increased. When the magnitude of evasive maneuver is given, the evasion problem changes to an optimal optimization problem of two control variables. In the following, we will introduce both analytical and numerical solutions to solve this problem.

3. The Relationship of Space Geometry

In this section, the relationship of relative space geometry and evasive maneuver is analyzed. Many different indexes have been used to describe the observability, such as the condition number of the observability matrix [24] and the distance error [25]. A new index that represents the level of state estimation is introduced here which is different from the previous indexes, and we call it measurement observability.

3.1. State Transfer Matrix for HEO. The relative Local Vertical Local Horizontal (LVLH) coordinate system is used as reference frame to describe orbital relative motion. Since pursuer and evader are in elliptical orbit, the Tschauner-Hempel (TH) equation [26] is introduced to describe the relative motion. The homogeneous solution is Yamanaka-Ankersen state transfer matrix [27]:

$$\begin{aligned}\mathbf{\Phi}(t,t_0) &= \begin{bmatrix} \mathbf{\Phi}_{rr}(t,t_0) & \mathbf{\Phi}_{rv}(t,t_0) \\ \mathbf{\Phi}_{vr}(t,t_0) & \mathbf{\Phi}_{vv}(t,t_0) \end{bmatrix} \\ &= \mathbf{\Phi}_{\theta}(f)\,\mathbf{\Phi}_{\theta}^{-1}(f_0),\end{aligned} \tag{1}$$

where f_0 and f are true anomaly of the reference spacecraft at t_0 and t, respectively. The expressions of $\mathbf{\Phi}_{\theta}(f)$ and $\mathbf{\Phi}_{\theta}^{-1}(f_0)$ are as follows:

$$\mathbf{\Phi}_{\theta}(f) = \left[\begin{array}{ccc|ccc} s & c & 2-3esI & 0 & 0 & 0 \\ s' & c' & -3e\left(sI+\dfrac{s}{k^2}\right) & 0 & 0 & 0 \\ c\left(1+\dfrac{1}{k}\right) & -s\left(1+\dfrac{1}{k}\right) & -3k^2 I & 1 & 0 & 0 \\ \hline -2s & e-2c & -3(1-2esI) & 0 & 0 & 0 \\ 0 & 0 & 0 & 0 & c & s \\ 0 & 0 & 0 & 0 & -s & c \end{array}\right],$$

$$\boldsymbol{\Phi}_{\theta}^{-1}(f_0) = \left[\begin{array}{ccc|ccc} -3s\dfrac{k+e^2}{k^2} & c-2e & 0 & -s\dfrac{k+1}{k} & 0 & 0 \\ -3\left(e+\dfrac{c}{k}\right) & -s & 0 & -\left(c\dfrac{k+1}{k}+e\right) & 0 & 0 \\ 3k-\lambda^2 & es & 0 & k^2 & 0 & 0 \\ \hline -3es\dfrac{k+1}{k^2} & -2+ec & \lambda^2 & -es\dfrac{k+1}{k} & 0 & 0 \\ 0 & 0 & 0 & 0 & \lambda^2 c & -\lambda^2 s \\ 0 & 0 & 0 & 0 & \lambda^2 s & \lambda^2 c \end{array}\right], \quad (2)$$

where $k = 1 + e\cos f$, $c = k\cos f$, $s = k\sin f$, $I = \int_{f_0}^{f}(1/k^2)du = (\mu^2/h^3)(t - t_0)$, $\lambda = \sqrt{1-e^2}$. e is eccentricity of the reference orbit, μ is gravitational coefficient of the earth, s' and c' are the first derivative of s and c with respect to f.

In the following, we set $\boldsymbol{\Phi}_p = [\boldsymbol{\Phi}_{rr} \quad \boldsymbol{\Phi}_{rv}]$ and $\mathbf{B} = [\boldsymbol{\Phi}_{rv} \quad \boldsymbol{\Phi}_{vv}]^{\mathrm{T}} = [\mathbf{B}_r \quad \mathbf{B}_v]^{\mathrm{T}}$. Assume a spacecraft executes a maneuver $\mathbf{u}$ at t_0; then the relative state at t with respect to the reference orbit is

$$\mathbf{X}_t = \boldsymbol{\Phi}(t, t_0)\,\mathbf{X}_{t_0} + \mathbf{B}\mathbf{u}. \quad (3)$$

3.2. Measurement Equations. In the actual projects, optical camera is one of the most common measuring devices and can provide two independent angle measurements (contains elevation ε and azimuth θ) at every moment. Figure 1 shows the geometric schematic of the orbital pursuit-evasion system along with the elevation and azimuth in the frame of camera, where F_{PO}, F_{MO}, and F_{EO} are the evader, pursuer, and camera coordinate systems, respectively. F_{MO} and F_{PO} are regarded as the same coordinate system in the following analysis. The definition of the orbital coordinate system is as follows: z is along the position vector which is from the center of the earth to the pursuer, x is perpendicular to z in the orbital plane and at the same side of the velocity direction, and $y = x \times z$ obeys the right-handed coordinate system. The definition of the orbital coordinate attached to the evader is omitted here, since the definition is similar.

The relative position between the evader and pursuer in measuring coordinate system is denoted as $\mathbf{r}_{PE} = [x \quad y \quad z]^{\mathrm{T}}$; the relationship of $\mathbf{r}_{PE}$ and measuring parameters obtained from the optical camera is

$$\mathbf{h}(\mathbf{X}_E) = \begin{bmatrix} \varepsilon \\ \theta \end{bmatrix} = \begin{bmatrix} \arctan\left(\dfrac{z_{PE}}{x_{PE}}\right) \\ \arctan\left(\dfrac{y_{PE}}{\sqrt{x_{PE}^2 + z_{PE}^2}}\right) \end{bmatrix}, \quad (4)$$

where ε and θ are the elevation and azimuth angles, respectively.

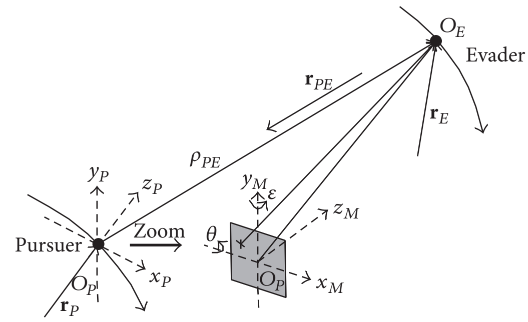

Figure 1: Relative observation geometry.

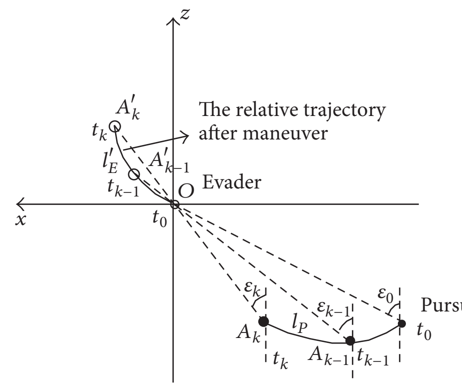

Figure 2: Completely unobservable maneuver.

Through linear inverse transformation, (4) is transferred to

$$\mathbf{H}(\mathbf{y})\,\mathbf{X}_r = 0, \quad (5)$$

where $\mathbf{X}_r$ is position component of the relative state and $\mathbf{H}(\mathbf{y})$ is as follows:

$$\mathbf{H}(\mathbf{y}) = \begin{bmatrix} \sin(\varepsilon) & 0 & -\cos(\varepsilon) \\ \sin(\theta) & -\cos(\varepsilon)\cos(\theta) & 0 \end{bmatrix}. \quad (6)$$

According to the EKF, the relative position and velocity can be estimated using the equations above during the angles-only relative navigation. It is easy to find that the maneuver of pursuer or evader will affect the relative navigation, measurement, and the observability of the system.

3.3. Space Geometry Analysis

Definition 1. Assume evader executes a nonzero evasive maneuver at t_0; if the angle measurements pursuer acquired after the evasive maneuver stays the same compared with those of no maneuver, then the evasive maneuver can be called completely unobservable maneuver.

Figure 2 shows the projection of relative motion trajectory in xz plane and describes the space geometry of completely unobservable maneuver. Assuming the evader's orbit without maneuvers as a reference orbit, then trajectories

l_P and l'_E describe the relative motion of the pursuer and of the evader when evasion maneuvers are exploited. In Figure 2, $\mathbf{A}_k\mathbf{O}$ represents the relative position vector of the pursuer, and $\mathbf{OA}'_k$ the relative position vector of the evader with an evasive maneuver, with respect to the reference orbit. Definition 1 can be illustrated as follows: the relative motion trajectory l'_E satisfies the geometry relationship described in Figure 2, namely, $\mathbf{A}_k\mathbf{O} = \lambda\mathbf{OA}'_k$, at any time after evasion ($k = 1, 2, 3, \ldots, \lambda$ is nonnegative). Thus, the angle measurements pursuer acquired after the evasive maneuver stays the same compared with those without evasion. In this situation, pursuer will never find out whether evader executes an evasive maneuver. When l'_E in Figure 2 exits from the scenario of the pursuer, the correspondent evasive maneuver $\mathbf{u}_E$ is called completely unobservable maneuver.

However, the completely unobservable maneuver is only a hypothesis about space geometry. After derivation, it can be found that the completely unobservable maneuver does not exist. We have the following.

Theorem 2. *If the initial relative distance of pursuer and evader is nonzero, the evasive maneuver evader executed cannot become completely unobservable maneuver.*

Proof. Assume a completely unobservable maneuver $\mathbf{u}_E$ exits. Set t_0 as initial time and take the initial two steps t_1 and t_2 as example. The relative position of evader after evasion and the reference orbit are as follows:

$$\begin{aligned} \mathbf{X}_{Er1} &= \mathbf{B}_r\mathbf{u}_E, \\ \mathbf{X}_{Er2} &= \mathbf{\Phi}_p\mathbf{B}\mathbf{u}_E. \end{aligned} \tag{7}$$

If the relative state of pursuer and the reference orbit is $\mathbf{X}_{P0}$ and the position component is nonzero, then

$$\begin{aligned} \mathbf{X}_{Pr1} &= \mathbf{\Phi}_p\mathbf{X}_{P0}, \\ \mathbf{X}_{Pr2} &= \mathbf{\Phi}_p^2\mathbf{X}_{P0}, \end{aligned} \tag{8}$$

where $\mathbf{\Phi}_p^2 = \mathbf{\Phi}_p\mathbf{\Phi}$, $\mathbf{X}_{Pr1}$ and $\mathbf{X}_{Pr2}$ are position vectors.

According to (5) and Definition 1, we have

$$\begin{aligned} \mathbf{H}(\mathbf{y}_1)\mathbf{X}_{Pr1} &= \mathbf{H}(\mathbf{y}_1)\mathbf{X}_{Er1} = 0, \\ \mathbf{H}(\mathbf{y}_2)\mathbf{X}_{Pr2} &= \mathbf{H}(\mathbf{y}_2)\mathbf{X}_{Er2} = 0; \end{aligned} \tag{9}$$

namely,

$$\begin{aligned} \mathbf{H}(\mathbf{y}_1)(\mathbf{B}_r\mathbf{u}_E) &= \mathbf{H}(\mathbf{y}_1)\left(\mathbf{\Phi}_p\mathbf{X}_{P0}\right) = 0, \\ \mathbf{H}(\mathbf{y}_2)\left(\mathbf{\Phi}_p\mathbf{B}\mathbf{u}_E\right) &= \mathbf{H}(\mathbf{y}_2)\left(\mathbf{\Phi}_p^2\mathbf{X}_{P0}\right) = 0; \end{aligned} \tag{10}$$

According to the property of solution space, it is easy to find out the following relation:

$$\mathbf{B}_r\mathbf{u}_E = \alpha_1\left(\mathbf{\Phi}_p\mathbf{X}_{P0}\right), \tag{11}$$

$$\mathbf{\Phi}_p\mathbf{B}\mathbf{u}_E = \alpha_2\left(\mathbf{\Phi}_p^2\mathbf{X}_{P0}\right), \tag{12}$$

where α_i is nonzero real number.

Therefore, if (11) and (12) are proved to be held, the existence of completely unobservable maneuver can be proved. □

From (11), we have

$$\mathbf{u}_E = \alpha_1\left(\mathbf{B}_r^{-1}\mathbf{\Phi}_p\mathbf{X}_{P0}\right). \tag{13}$$

Substitute (13) into (12) and take the second step of (12) into consideration; then

$$\begin{aligned} \mathbf{\Phi}_p\left(\kappa_1\mathbf{\Phi} - \mathbf{B}\mathbf{B}_r^{-1}\mathbf{\Phi}_p\right)\mathbf{X}_{P0} &= 0, \\ \mathbf{\Phi}_p^2\left(\kappa_2\mathbf{\Phi} - \mathbf{B}\mathbf{B}_r^{-1}\mathbf{\Phi}_p\right)\mathbf{X}_{P0} &= 0, \end{aligned} \tag{14}$$

where $\kappa_i = \alpha_{i+1}/\alpha_i$.

Since $\mathbf{\Phi}_p$ is linear transformation and (14) do hold, the necessary and sufficient condition of the nonzero solution existence of $\mathbf{X}_{P0}$ is $\kappa_1 = \kappa_2 \equiv \kappa$ (the initial relative position is nonzero). Thus,

$$\mathbf{\Phi}_p\left(\kappa\mathbf{\Phi} - \mathbf{B}\mathbf{B}_r^{-1}\mathbf{\Phi}_p\right)\mathbf{X}_{P0} = 0. \tag{15}$$

In addition, if the nonzero solution of $\mathbf{X}_{P0}$ exists, according to the existence theorem of solutions of linear equation, we can acquire $\operatorname{rank}(\kappa\mathbf{\Phi} - \mathbf{B}\mathbf{B}_r^{-1}\mathbf{\Phi}_p) < 6$. Expand $(\kappa\mathbf{\Phi} - \mathbf{B}\mathbf{B}_r^{-1}\mathbf{\Phi}_p)$ and one can get

$$\begin{aligned} &\left(\kappa\mathbf{\Phi} - \mathbf{B}\mathbf{B}_r^{-1}\mathbf{\Phi}_p\right) \\ &= \begin{bmatrix} (\kappa-1)\mathbf{\Phi}_{11} & (\kappa-1)\mathbf{\Phi}_{12} \\ \kappa\mathbf{\Phi}_{21} - \mathbf{\Phi}_{22}\mathbf{\Phi}_{12}^{-1}\mathbf{\Phi}_{11} & (\kappa-1)\mathbf{\Phi}_{22} \end{bmatrix}. \end{aligned} \tag{16}$$

Because $\operatorname{rank}(\mathbf{\Phi}) = 6$, it is easy to know that if and only if $\beta = 1$ the expression $\operatorname{rank}(\kappa\mathbf{\Phi} - \mathbf{B}\mathbf{B}_r^{-1}\mathbf{\Phi}_p) < 6$ can be held. Equation (15) is revised as

$$\mathbf{\Phi}_p\left(\mathbf{\Phi} - \mathbf{B}\mathbf{B}_r^{-1}\mathbf{\Phi}_p\right)\mathbf{X}_{P0} = 0. \tag{17}$$

Substitute $\kappa = 1$ into (16), then

$$\begin{aligned} &\begin{bmatrix} (\kappa-1)\mathbf{\Phi}_{11} & (\kappa-1)\mathbf{\Phi}_{12} \\ \kappa\mathbf{\Phi}_{21} - \mathbf{\Phi}_{22}\mathbf{\Phi}_{12}^{-1}\mathbf{\Phi}_{11} & (\kappa-1)\mathbf{\Phi}_{22} \end{bmatrix} \\ &= \begin{bmatrix} \mathbf{0} & \mathbf{0} \\ \mathbf{\Phi}_{21} - \mathbf{\Phi}_{22}\mathbf{\Phi}_{12}^{-1}\mathbf{\Phi}_{11} & \mathbf{0} \end{bmatrix}. \end{aligned} \tag{18}$$

Set $\mathbf{X}_{P0} = [\mathbf{X}_{Pr0} \quad \mathbf{X}_{Pv0}]^{\mathrm{T}}$. It can be seen from (17) and (18) that the value of $\mathbf{X}_{Pv0}$ makes no influence on the result of (17). When $\mathbf{X}_{Pr0}$ is arbitrary, the equalities do not always hold. Furthermore, (17) always holds only when $\mathbf{X}_{Pr0} = 0$. This condition goes with the antecedent hypothesis of *Theorem 2*; therefore *Theorem 2* is proved in this way. Unobservable maneuvers proofs have previously been developed for the bearings-only navigation problem in circular orbit [21]; here the related conclusion is extended to elliptical orbit successfully.

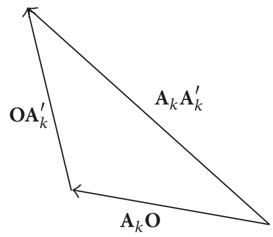

Figure 3: The components of measuring line of sight.

Though the completely unobservable maneuver is nonexistent, it is set under the situation of ideal measurement. In reality, if the angle measurements pursuer acquired after the evasive maneuver stays quite close to those of no maneuver and the difference approach to the measurement accuracy, pursuer could be unable to identify the evasive maneuver. Thus, these evasive maneuvers can be called approximate solution of the completely unobservable maneuver. It can be said that the difficulty of maneuver tracking for pursuer is increased when the difference of angle measurements the evasion caused is decreased. This is a new index to evaluate the superiority of an evasive maneuver.

4. Optimal Evasion Maneuvers Analysis

In this section, an analytical solution is derived based on the conclusion of Section 3 and meanwhile a numerical solution is given to prove the optimality of analytical solution.

4.1. Analytical Solution

4.1.1. Quantification of Space Geometry. To find the optimal evasive maneuver, it is necessary to quantify the relationship of angle measurements variation and space geometry of pursuer and evader. In Euclidean space, orthogonality between two vectors can be defined by using the notion dot product. Thus, two column unit vectors $\mathbf{a}$ and $\mathbf{b}$ are orthogonal when $\mathbf{a}^{\mathrm{T}} \cdot \mathbf{b} = 0$. On the contrary, if the scalar product of $\mathbf{a}$ and $\mathbf{b}$ is 1 or −1 ($\mathbf{a}^{\mathrm{T}} \cdot \mathbf{b} = 1$ or $\mathbf{a}^{\mathrm{T}} \cdot \mathbf{b} = -1$), then $\mathbf{a}$ and $\mathbf{b}$ are parallel.

From Figure 2 we know that $\mathbf{A}_k\mathbf{O}$ is the measuring line of sight of pursuer and the reference orbit, $\mathbf{A}_k\mathbf{A}'_k$ is the measuring line of sight of pursuer and evader after evasion. To each measuring time, the norm of $\mathbf{A}_k\mathbf{O}$ and $\mathbf{A}_k\mathbf{A}'_k$ is constant. Therefore, in order to decrease the variation of angle measurements caused by evasion, the included angle of $\mathbf{A}_k\mathbf{A}'_k$ and $\mathbf{A}_k\mathbf{O}$ must be as small as possible. As an extreme example, when the included angle of $\mathbf{A}_k\mathbf{A}'_k$ and $\mathbf{A}_k\mathbf{O}$ is 0 or $-\pi$, the evasive maneuver becomes the completely unobservable maneuver.

Since the norm of $\mathbf{A}_k\mathbf{A}'_k$ and $\mathbf{A}_k\mathbf{O}$ is definite value, if the evasive maneuver is optimal, the scalar product of $\mathbf{A}_k\mathbf{A}'_k$ and $\mathbf{A}_k\mathbf{O}$ should be maximum. It is seen from Figures 2 and 3 that the measuring line of sight $\mathbf{A}_k\mathbf{A}'_k$ can be expressed as

$$\mathbf{A}_k\mathbf{A}'_k = \mathbf{A}_k\mathbf{O} + \mathbf{OA}'_k. \tag{19}$$

At k time, the scalar product of $\mathbf{A}_k\mathbf{A}'_k$ and $\mathbf{A}_k\mathbf{O}$ is

$$\begin{aligned}\mathbf{A}_k\mathbf{O}^{\mathrm{T}} \cdot \mathbf{A}_k\mathbf{A}' &= \mathbf{A}_k\mathbf{O}^{\mathrm{T}} \cdot \left(\mathbf{A}_k\mathbf{O} + \mathbf{OA}'_k\right) \\ &= \mathbf{A}_k\mathbf{O}^{\mathrm{T}} \cdot \mathbf{A}_k\mathbf{O} + \mathbf{A}_k\mathbf{O}^{\mathrm{T}} \cdot \mathbf{OA}'_k.\end{aligned} \tag{20}$$

It is easy to know that the value of $\mathbf{A}_k\mathbf{O}^{\mathrm{T}} \cdot \mathbf{A}_k\mathbf{O}$ is constant at each time; thus the scalar product of $\mathbf{A}_k\mathbf{A}'_k$ and $\mathbf{A}_k\mathbf{O}$ is decided by $\mathbf{A}_k\mathbf{O}^{\mathrm{T}} \cdot \mathbf{OA}'_k$. Therefore, to minimize the variation of angle measurements at k time, the optimization at k time should minimize the following object:

$$J_k = -\mathbf{A}_k\mathbf{O}^{\mathrm{T}} \cdot \mathbf{OA}'_k. \tag{21}$$

According to the relationship of evasive maneuver and space geometry, (21) can be revised as

$$J_k = -\left(\mathbf{\Phi}_P \mathbf{X}_{P0}\right)^{\mathrm{T}} \cdot \mathbf{B}_r \mathbf{u}. \tag{22}$$

During the approaching, the optimal evasion should minimize the object J_k at every moment; thus the object function of the whole approaching is as follows:

$$J = \sum_{k=0}^{N} J_k = -\sum_{k=0}^{N} \left(\mathbf{\Phi}_P \left(t_k, t_0\right) \mathbf{X}_{P0}\right)^{\mathrm{T}} \cdot \mathbf{B}_r \left(t_k, t_0\right) \mathbf{u}, \tag{23}$$

where N is the number of measurements.

Equation (23) shows that the evasive effectiveness is not only dependent on the maneuvers performed by $\mathbf{u}$ but also dependent on the position where they are executed. Since this equation is closed form, it allows for simple inclusion inside a global trajectory optimization scheme as an additional objective or independent objective, weighed by other objective such as relative distance or fuel consumption. This would permit a global trajectory optimizer to choose maneuvers that will increase the difficulty of maneuver tracking for pursuer. It is worth noting that (23) provides explicit solutions for any arbitrary set of initial conditions (nonzero initial relative position).

4.2. Algebraic Optimal Evasive Maneuver. To find the optimal evasive maneuver for a constant duration of measurement, the optimization variable of interest in (23) is the evasive maneuver $\mathbf{u}$. The initial state $\mathbf{X}_{P0}$ is fixed when the evasive maneuver is executed. N is the number of measurements.

Since (23) is a linear function for evasive maneuver, it can only be minimized with respect to $\mathbf{u}$. After the former quantification analysis above, the optimal evasive maneuver can be found based on (23). It is logical to limit the desired evasive maneuver $\mathbf{u}$ magnitude s in order to find the optimal evasive maneuver direction. Then, this constraint can be mathematically posed as follows:

$$\chi(\mathbf{u}) = \mathbf{u}^{\mathrm{T}}\mathbf{u} - s^2 = 0. \tag{24}$$

It should be noted that additional constraints could be considered here, if it is needed. Closed form solutions would be possible by the following steps with constraints mentioned above.

The constrained optimization problem transfers to minimize (23) with respect to the evasive maneuver $\mathbf{u}$, under the equality constraint proposed by (24). Since there is no inequality constraint in this problem, it can be converted to an equivalent unconstrained problem with the Lagrange multiplier technique used in [28]. The problem is converted to minimize the Lagrangian function

$$\Gamma(\mathbf{u}, \lambda) = J(\mathbf{u}) - \lambda\chi(\mathbf{u}) = 0, \tag{25}$$

where λ is the Lagrange multiplier corresponding to the equality constrain in (24).

The first-order optimality conditions are given by the derivatives of the Lagrangian function with respect to the optimization variables equal to zero, as well as the Lagrange multiplier. Thus, we have

$$\begin{aligned} \frac{\partial\Gamma}{\partial\mathbf{u}} &= -\sum_{k=0}^{N}\left(\mathbf{\Phi}_P(t_k, t_0)\mathbf{X}_{P0}\right)^{\mathrm{T}}\mathbf{B}_r(t_k, t_0) - 2\lambda\mathbf{u}^{\mathrm{T}} = 0, \\ \frac{\partial\Gamma}{\partial\lambda} &= \mathbf{u}^{\mathrm{T}}\mathbf{u} - s^2 = 0. \end{aligned} \tag{26}$$

According to (26), we have

$$\begin{aligned} \mathbf{u} &= -\frac{\sum_{k=0}^{N}\mathbf{B}_r^{\mathrm{T}}(t_k, t_0)\left(\mathbf{\Phi}_P(t_k, t_0)\mathbf{X}_{P0}\right)}{2\lambda}, \\ \lambda &= \pm\frac{1}{2s}\sqrt{\sum_{k=0}^{N}\left(\mathbf{\Phi}_P(t_k, t_0)\mathbf{X}_{P0}\right)^{\mathrm{T}}\mathbf{B}_r(t_k, t_0)\sum_{k=0}^{N}\mathbf{B}_r^{\mathrm{T}}(t_k, t_0)\left(\mathbf{\Phi}_P(t_k, t_0)\mathbf{X}_{P0}\right)}. \end{aligned} \tag{27}$$

Take the second-order optimality conditions into consideration in order to identify the stationary point corresponding to the minimum of the Lagrangian function.

$$\begin{aligned} \frac{\partial^2\Gamma}{\partial\mathbf{u}^2} &= -2\lambda > 0 \longrightarrow \\ \lambda &< 0. \end{aligned} \tag{28}$$

According to (27) and (28), an algebraic expression for optimal evasive maneuver $\mathbf{u}_{\mathrm{opt}}$ can be obtained as follows:

$$\mathbf{u}_{\mathrm{opt}} = -s\frac{\sum_{k=0}^{N}\mathbf{B}_r^{\mathrm{T}}(t_k, t_0)\left(\mathbf{\Phi}_P(t_k, t_0)\mathbf{X}_{P0}\right)}{\sqrt{\sum_{k=0}^{N}\left(\mathbf{\Phi}_P(t_k, t_0)\mathbf{X}_{P0}\right)^{\mathrm{T}}\mathbf{B}_r(t_k, t_0)\sum_{k=0}^{N}\mathbf{B}_r^{\mathrm{T}}(t_k, t_0)\left(\mathbf{\Phi}_P(t_k, t_0)\mathbf{X}_{P0}\right)}}. \tag{29}$$

Equation (29) is the analytical expression of optimal evasive maneuver including the initial states $\mathbf{x}0$ and the expectable evasive maneuver magnitude s. Till now, the expression of the analytical solution is obtained, and it provides the optimal evasive maneuver with respect to relative space geometry and the angle measurements. The state transition $\mathbf{\Phi}_p$ and input transition $\mathbf{B}_r$ were proposed in Section 3.

4.3. Numerical Solution. In order to prove the optimality of analytical solution, an optimization model is established in this section. One of the most well-known evolutionary algorithms, GA, is employed to solve the optimization problem. The GA has been successfully applied in spacecraft trajectory optimization, for example, in designing low-thrust trajectories [29] and solving two different kinds of problems typical to astrodynamics [30].

Optimization Variables. Since the desired evasive maneuver ΔV magnitude is limited to s, in order to find the optimal direction of evasive maneuver, azimuth θ and elevation ε are selected as two optimization variables; namely,

$$\mathbf{D} = [\varepsilon, \theta]^{\mathrm{T}}. \tag{30}$$

In consideration of the space geometric relationship between evader and pursuer, the constraint conditions for an orbital evasion problem read

$$\begin{aligned} -2\pi &\le \varepsilon \le 2\pi, \\ -\pi &\le \theta \le \pi. \end{aligned} \tag{31}$$

In order to further simplify the problem, here we focus on the value range of the optimization variables. For two satellites in orbit, it is known from [19] that an increased difference of the system relative motion has a positive correlation with system observability. Therefore, if the initial orbit is coplanar, the evasive maneuver should better be coplanar, too.

Under such circumstance, new constraint conditions are as stated in the following:

$$-2\pi \le \varepsilon \le 2\pi,$$
$$|\theta| \le \xi, \quad \xi = 0.01. \tag{32}$$

Objective Function. Assume that $\overline{\mathbf{A}_k\mathbf{O}}$ and $\overline{\mathbf{OA}'_k}$ are the unit vectors of $\mathbf{A}_k\mathbf{O}$ and $\mathbf{OA}'_k$, separately. According to Section 4.1, it is easy to know that the closer to 1 the value of $\overline{\mathbf{A}_k\mathbf{O}}\cdot\overline{\mathbf{OA}'_k}$ is, the smaller the variation of angle measurements is. During the measurement, when the sum of $\overline{\mathbf{A}_k\mathbf{O}}\cdot\overline{\mathbf{OA}'_k}$ is max, the evasive maneuver is optimal. Thus, objective function is as follows:

$$\max_{\mathbf{u}} f(\mathbf{u}) = \sum_{k=0}^{N} \overline{\mathbf{A}_k\mathbf{O}} \cdot \overline{\mathbf{OA}'_k}, \tag{33}$$

where $\overline{\mathbf{A}_k\mathbf{O}}$ and $\overline{\mathbf{OA}'_k}$ are equal to the unit vector of $\mathbf{\Phi}_p(t_k, t_0)\mathbf{X}_{P0}$ and $\mathbf{B}_r(t_k, t_0)\mathbf{u}$.

In order to use GA, the objective function is revised as

$$\min_{\mathbf{u}} f(\mathbf{u}) = -\sum_{k=0}^{N} \overline{\mathbf{A}_k\mathbf{O}} \cdot \overline{\mathbf{OA}'_k}. \tag{34}$$

Thus, the GA optimization model is established. Through the results comparison of analytical and numerical solutions, the optimality of analytical solution can be proved.

5. Simulation

Simulation results are presented in this section. Consider an illustrative example: evader is in a HEO and semimajor axis is 45485189 m, eccentricity is 0.713, inclination of orbit is 1.10187 rad, right ascension of ascending node (RAAN) is 0.84489 rad, argument of perigee is 4.7022 rad, and true anomaly is 1.4856 rad. Assume that the initial time is $t_0 = 0$, and initial relative states $\mathbf{X}_{P0}$ at t_0 is

$$\mathbf{X}_{P0} = [-85204.071\,\text{m}, -47965.164\,\text{m}, 0, 16.845\,\text{m/s}, 4.306\,\text{m/s}, 0.0]^{\mathrm{T}}. \tag{35}$$

The pursuer uses optical camera to get relative measurements. The measurement frequency of the optical camera is assumed as 0.1 Hz. The magnitude of evasive impulse is fixed to 3 m/s (namely, $s = 3$ m/s). The optimization parameters of GA are as follows: 100 for population size; 30 for maximum generations number; 0.90 for crossover probability; and 0.08 for mutation probability. Constraint conditions are chosen as those in Section 4.2.

If the evasion is aimed at 101 angle measurements, then the measuring time is 1000 s. It is easy to know that the minimum value of objective function should be −101. Thus, the optimization results are obtained in Figure 4.

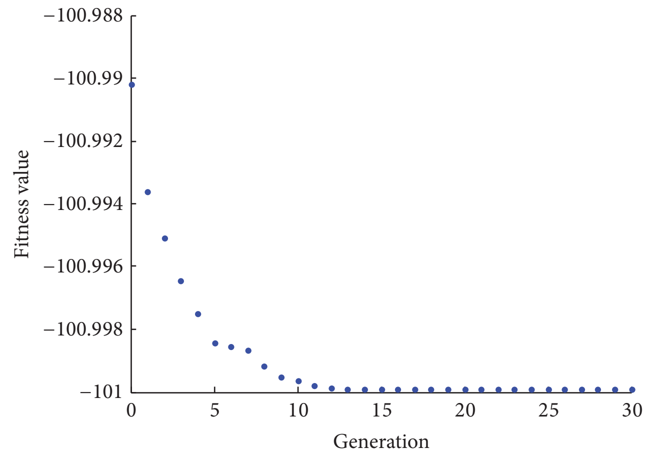

Figure 4: The optimization results of GA.

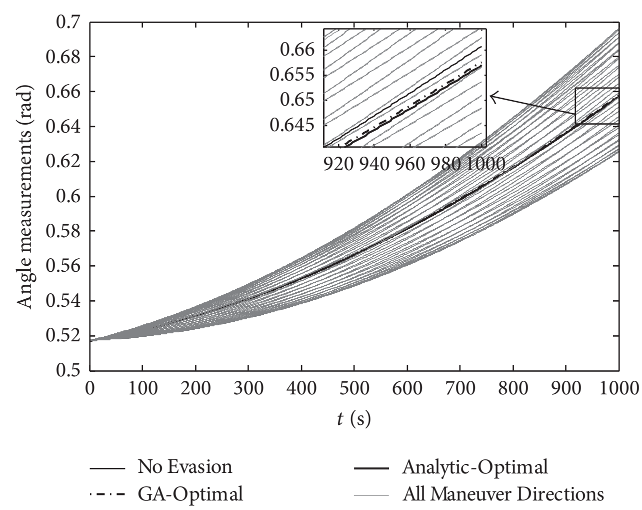

Figure 5: Angle measurements in 1000 s.

It can be seen from Figure 4 that the numerical solution is −100.9998. After 15 generations, the results reach convergence. The direction of optimal evasive maneuver is $\mathbf{D}_{V\text{opt}} = [-2.4031, 0]^{\mathrm{T}}$. Take correlated parameters into (29), the analytical solution is acquired and the direction of analytical evasive maneuver is $\mathbf{D}_{V\text{analytical}} = [-2.4219, 0]^{\mathrm{T}}$.

The measurement effectiveness of the optimal evasive maneuvers is validated by comparing the GA-optimal and analytical-optimal evasive maneuvers to the propagation of 80 different maneuver directions, covering ε from -2π to 2π. The angle measurements during the previous 1000 s are shown in Figure 5.

Set the angle measurements of reference orbit as reference measurements. The angle measurements with an evasive maneuver at each time minus reference measurements become the variation of angle measurements. The variation of angle measurements during the previous 1000 s is given in Figure 6.

As seen from Figure 6, the variation of angle measurements caused by the GA-optimal and analytical-optimal

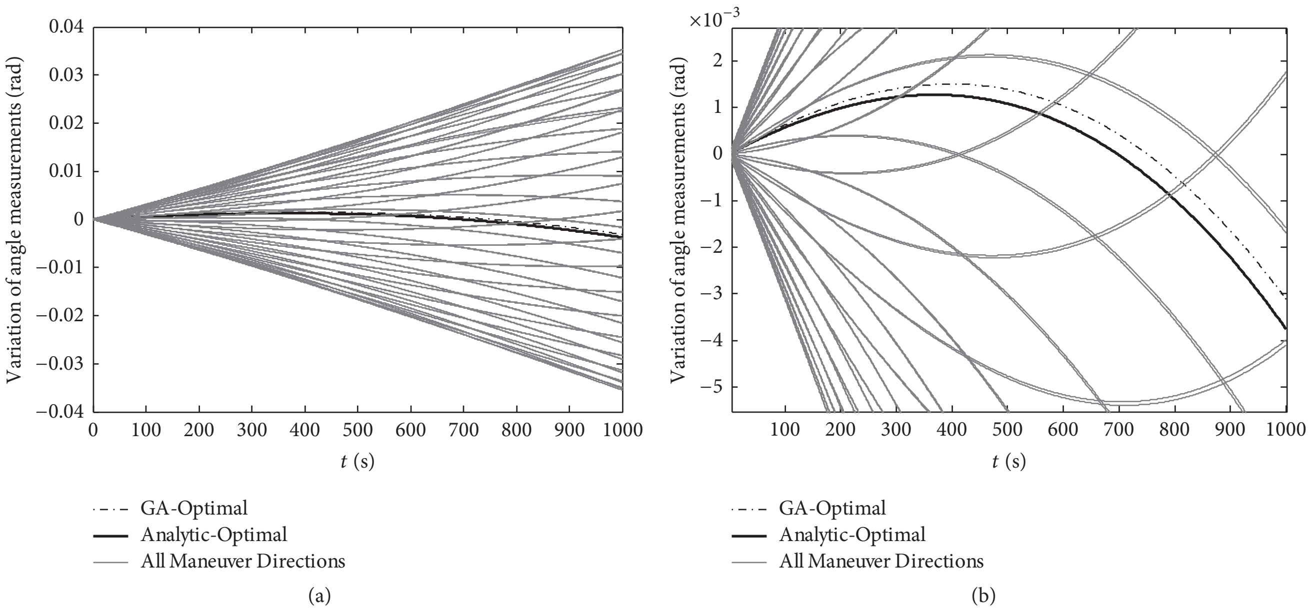

Figure 6: The variation of angle measurements due to optimal maneuvers (a) and zoom (b).

solutions are much smaller than other maneuver directions. Although the analytical-optimal variation of angle measurements at the end time is bigger than that of GA-optimal, the sum of the variation is optimal for the whole measuring time. It can be seen that the variation of angle measurements caused by the analytical-optimal solution is no more than 0.001 rad for the previous 800 s, which means that the pursuer will even not find out the evasion if the measurement accuracy is not better than 0.001 rad.

In order to show that the proposed analytical and numerical maneuvers provide the most guidance error in the filter estimate, a Kalman filter is used as the navigation filter. The simulation conditions are the same with the simulation in Figures 4–6, and the initial guidance error is assumed to be nonzero. The simulation step is set to 5 s. The guidance error of the optimal evasive maneuvers is validated by comparing the GA-optimal and analytical-optimal evasive maneuvers to the propagation of 60 different maneuver directions, covering ε from -2π to 2π. The guidance errors in the two directions of orbit plane are shown in Figures 7 and 8.

As Figures 7 and 8 show, the analytical and numerical maneuvers provide the most improvement of guidance error. Though the guidance error caused by the analytical maneuvers is better than that of numerical maneuvers, the difference is minor. The simulation results show that the analytical analysis in Section 4 is effective. Moreover, since the solution is analytical, it will have a potential application in engineering utilization.

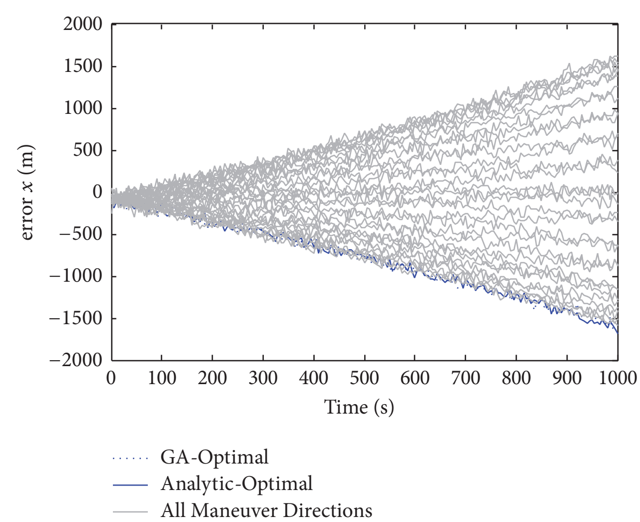

Figure 7: Navigation errors caused by maneuvers (Dircetion x).

6. Conclusions

An analytical optimal evasion strategy is proposed for an evading satellite against a noncooperative rendezvous spacecraft. This work extends the research objective to not only orbit debris but also spacecraft with maneuver ability. Through analysis of relative space geometry, the completely unobservable maneuver is defined and proved to be nonexistent. An analytical closed-form solution is proposed to compute optimal evasive maneuvers for angles-only navigation. Based on this analytical method, an optimal evasive maneuver can be quickly obtained. Since the previous evasion strategies required numerical optimization which a lot of time is needed, the method in this work should be an effective improvement compared with the previous evasion state of art. Moreover, in order to decline the navigation accuracy of pursuer, the relative space geometry is analyzed and quantified. Though the derivation is under the situation of HEO, it is also adaptable for orbital evasion problem in circular orbit.

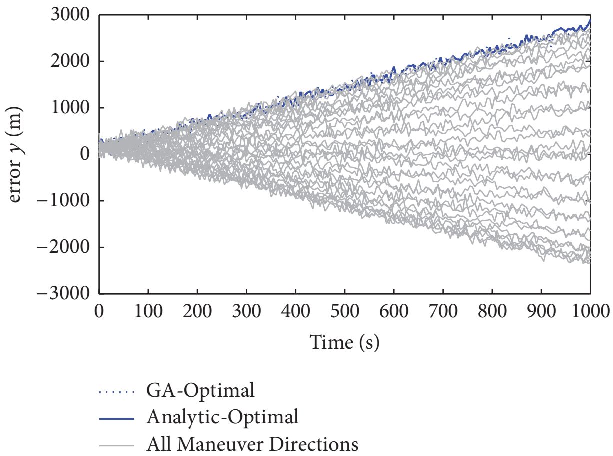

Figure 8: Navigation errors caused by maneuvers (Dircetion y).

This work proves that the angle measurements and navigation accuracy can be used in orbital evasion problem, which is often neglected in previous research. This research proposes a new research method that means a potential step closer to engineering utilization.

Conflicts of Interest

The authors declare that they have no conflict of interests.

Acknowledgments

Project is supported by the National Natural Science Foundation of China (Grant no. 11572345).

References

[1] J. Shinar, Y. Rotsztein, and E. Bezner, "Analysis of three-dimensional optimal evasion with linearized kinematics," *Journal of Guidance, Control, and Dynamics*, vol. 2, no. 5, pp. 353–360, 1979.

[2] I. Forte, A. Steinberg, and J. Shinar, "The effects of non–linear kinematics in optimal evasion," *Optimal Control Applications and Methods*, vol. 4, no. 2, pp. 139–152, 1983.

[3] N. Sánchez-Ortiz, M. Belló-Mora, and H. Klinkrad, "Collision avoidance manoeuvres during spacecraft mission lifetime: risk reduction and required ΔV," *Advances in Space Research*, vol. 38, no. 9, pp. 2107–2116, 2006.

[4] T. Shima, "Optimal cooperative pursuit and evasion strategies against a homing missile," *Journal of Guidance, Control, and Dynamics*, vol. 34, no. 2, pp. 414–425, 2011.

[5] K. Chan, "Spacecraft maneuvers to mitigate potential collision threats," in *Proceedings of the Astrodynamics Specialist Conference and Exhibit (AIAA/AAS '02)*, Monterey, Calif, USA, August 2002.

[6] H.-D. Kim and H.-J. Kim, "Optimal collision avoidance maneuver to maintain a LEO station keeping," in *Proceedings of the 61st International Astronautical Congress (IAC '10)*, pp. 3056–3060, International Astronautical Federation (IAF), Prague, Czech Republic, October 2010.

[7] J. Shinar and D. Steinberg, "Analysis of optimal evasive maneuvers based on a linearized two-dimensional kinematic model," *Journal of Aircraft*, vol. 14, no. 8, pp. 795–802, 1977.

[8] I. Forte, A. Steinberg, and J. Shinar, "The effects of non-linear kinematics in optimal evasion," *Optimal Control Applications and Methods*, vol. 4, no. 2, pp. 139–152, 1983.

[9] B. D. Kelly and S. D. Picciotto, "Probability based optimal collision avoidance maneuvers," AIAA 2005-6775, 2005.

[10] R. P. Patera, "General method for calculating satellite collision probability," *Journal of Guidance, Control, and Dynamics*, vol. 24, no. 4, pp. 716–722, 2001.

[11] R. P. Patera and G. E. Peterson, "Space vehicle maneuver method to lower collision risk to an acceptable level," *Journal of Guidance, Control, and Dynamics*, vol. 26, no. 2, pp. 233–237, 2003.

[12] R. P. Patera, "Satellite collision probability for nonlinear relative motion," *Journal of Guidance, Control, and Dynamics*, vol. 26, no. 5, pp. 728–733, 2003.

[13] C. Bombardelli, "Analytical formulation of impulsive collision avoidance dynamics," *Celestial Mechanics and Dynamical Astronomy*, vol. 118, no. 2, pp. 99–114, 2014.

[14] S.-C. Lee, H.-D. Kim, and J. Suk, "Collision avoidance maneuver planning using GA for LEO and GEO satellite maintained in keeping area," *International Journal of Aeronautical and Space Sciences*, vol. 13, no. 4, pp. 474–483, 2012.

[15] E. H. Kim, H. D. Kim, and H. J. Kim, "Optimal solution of collision avoidance maneuver with multiple space debris," *Journal of Space Operations—Letters*, vol. 9, no. 3, pp. 20–31, 2012.

[16] A. D. de Jesus and R. R. de Sousa, "Processing optimized for symmetry in the problem of evasive maneuvers," *Computational & Applied Mathematics*, vol. 34, no. 2, pp. 521–534, 2015.

[17] S. E. Hammel and V. J. Aidala, "Observability Requirements for Three-Dimensional Tracking via Angle Measurements," *IEEE Transactions on Aerospace and Electronic Systems*, vol. 21, no. 2, pp. 200–207, 1985.

[18] S. C. Nardone and V. J. Aidala, "Observability criteria for bearings-only target motion analysis," *Institute of Electrical and Electronics Engineers. Transactions on Aerospace and Electronic Systems*, vol. 17, no. 2, pp. 162–166, 1981.

[19] D. A. Vallado, "Evaluating gooding angles-only obit determination of space based space surveillance measurements," in *Proceedings of the AAS Born Symposium*, Boulder, Colo, USA, May 2010.

[20] D. C. Woffinden and D. K. Geller, "Observability criteria for angles-only navigation," *IEEE Transactions on Aerospace and Electronic Systems*, vol. 45, no. 3, pp. 1194–1208, 2009.

[21] J. Grzymisch and W. Fichter, "Observability criteria and unobservable maneuvers for in-orbit bearings-only navigation," *Journal of Guidance, Control, and Dynamics*, vol. 37, no. 4, pp. 1250–1259, 2014.

[22] J. Grzymisch and W. Fichter, "Analytic optimal observability maneuvers for in-orbit bearings-only rendezvous," *Journal of Guidance, Control, and Dynamics*, vol. 37, no. 5, pp. 1658–1664, 2014.

[23] Y. Dateng, Y. Luo, J. Zicheng, and G. Tang, "Multi-objective evolutionary optimization of evasive maneuvers including observability performance," in *Proceedings of the IEEE Congress on Evolutionary Computation (CEC '15)*, pp. 603–610, Sendai, Japan, May 2015.

[24] D. C. Woffinden and D. K. Geller, "Optimal orbital rendezvous maneuvering for angles-only navigation," *Journal of Guidance, Control, and Dynamics*, vol. 32, no. 4, pp. 1382–1387, 2009.

[25] W. Fehse, *Automated Rendezvous and Docking of Spacecraft*, Cambridge University Press, Cambridge, UK, 2003.

[26] K. Alfriend, S. R. Vadali, and P. Gurfil, *Spacecraft Formation Flying: Dynamics, Control and Navigation*, vol. 2, Butterworth-Heinemann, Oxford, UK, 2009.

[27] K. Yamanaka and F. Ankersen, "New state transition matrix for relative motion on an arbitrary elliptical orbit," *Journal of Guidance, Control, and Dynamics*, vol. 25, no. 1, pp. 60–66, 2002.

[28] S. Boyd and L. Vandenberghe, *Convex optimization*, Cambridge University Press, Cambridge, UK, 2004.

[29] G. A. Rauwolf and V. L. Coverstone-Carroll, "Near-optimal low-thrust orbit transfers generated by a genetic algorithm," *Journal of Spacecraft and Rockets*, vol. 33, no. 6, pp. 859–862, 1996.

[30] G. Taini, L. Amorosi, A. Notarantonio, and G. B. Palmerini, "Applications of genetic algorithms in mission design," in *Proceedings of the IEEE Aerospace Conference*, 902, 890 pages, IEEE, Big Sky, Mont, USA, March 2005.

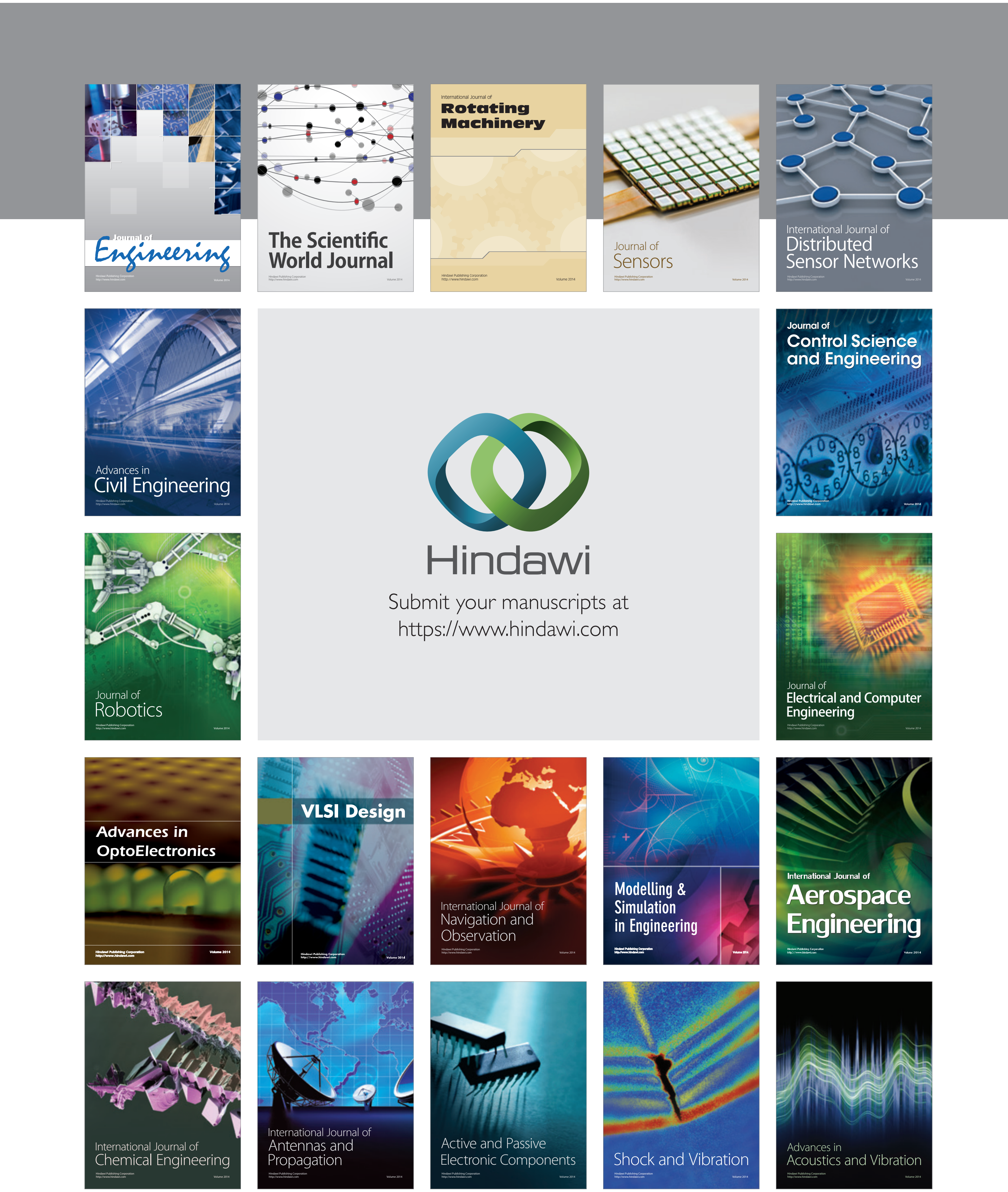

Journal of Engineering
The Scientific World Journal
International Journal of Rotating Machinery
Journal of Sensors
International Journal of Distributed Sensor Networks
Advances in Civil Engineering
Hindawi
Submit your manuscripts at
https://www.hindawi.com
Journal of Control Science and Engineering
Journal of Robotics
Journal of Electrical and Computer Engineering
Advances in OptoElectronics
VLSI Design
International Journal of Navigation and Observation
Modelling & Simulation in Engineering
International Journal of Aerospace Engineering
International Journal of Chemical Engineering
International Journal of Antennas and Propagation
Active and Passive Electronic Components
Shock and Vibration
Advances in Acoustics and Vibration